Trans. JSASS Aerospace Tech. Japan
Vol. 14, No. ists31, pp.Pd_1 - Pd_10, 2017

ISTS-2017-d-031／ISSFD-2017-031

Reliability Analysis of Ballistic Landing in Binary Asteroid 65803 (1996GT) Didymos under Uncertainty and GNC Error Considerations

By Onur CELIK,[1)] Ozgur KARATEKIN,[2)] Birgit RITTER[2)] and Joan Pau SANCHEZ[3)]

[1)] *Department of Space and Astronautical Science, The Graduate University for Advanced Studies (SOKENDAI), Sagamihara, Japan*
[2)] *Reference Systems and Planetology, the Royal Observatory of Belgium (ROB), Brussels, Belgium*
[3)] *Space Research Centre, School of Aerospace, Transport & Manufacturing, Cranfield University, Cranfield, United Kingdom*

(Received April 17, 2017)

Near-Earth asteroids are crucial to understand the formation of our solar system, furthermore they have been identified as resources for valuable raw materials and a threat to earthly life in the event of an impact. As remote sensing techniques capture the finest details of those during missions, in-situ investigations may provide the "ground-truth" and enhance the scientific return. Unpowered "science packages" have already been used in asteroid missions and are considered for future missions. A good example of their potential use can be seen in ESA's current mission study Asteroid Impact Mission (AIM). AIM is considering to carry along two CubeSats to be deployed in binary asteroid Didymos; one of which, ROB-led AGEX CubeSat project is proposed to land ballistically on the smaller companion (Didymoon). Ballistic soft landing opportunities in binary asteroids are demonstrated previously within the framework of Circular Restricted Three-Body Problem (CR3BP). The research here considers Didymoon the target body to land on, and addresses the impact of uncertainties on the landing trajectory by means of Monte Carlo simulation. Main uncertainties considered include mothership GNC errors, deployment system uncertainties, and the density uncertainties of Didymoon. The success criteria for the simulation is touchdown. Deployment altitude has a degrading effect on the success significantly. For the same altitude, the velocity-based uncertainties are dominant compared to their position-based counterparts. Success rates over 99.7% is achieved, though it may put extra requirements in mothership development.

Key Words: binary asteroids, the circular restricted three body problem, ballistic soft landing, Monte Carlo simulation

Nomenclature

CoR	:	coefficient of restitution
d	:	distance
v	:	velocity
$\boldsymbol{v}$	:	velocity vector
$\hat{\boldsymbol{n}}$	:	normal vector
r	:	radius
α	:	azimuth
λ	:	longitude
ϕ	:	elevation
σ	:	standard deviation of the mean
Subscripts		
barycentre	:	barycentre related
d	:	deployment related
deployment	:	deployment related
L2	:	L2 point related
landing	:	landing related
LV	:	local vertical
min	:	minimum
moon	:	Didymoon related
safe	:	safe
SC	:	spacecraft related
spring	:	spring related
u	:	uncertain
Superscripts		
$-$	:	incoming
$+$	:	outgoing

1. Introduction

Binary asteroids constitute a considerable portion of near-Earth asteroid population, about 15% according to recent estimates.[1)] Among variety of missions proposed to asteroids, or to small bodies in general, the interest on binary asteroids also seems to grow. Within the last decade, example proposals included Marco Polo-R, Binary Asteroid in-situ Exploration (BASiX), and Asteroid Impact and Deflection Assessment (AIDA).[2–4)] However, since the first and only ever visit of Galileo spacecraft to binary asteroid Ida-Dactyl, no mission aimed for the binaries.

Apart from scientific curiosity, and its escalating commercial value, asteroid exploration is also important for its potential impact risk to the Earth. The threat is taken seriously and a variety of techniques is proposed to deflect potentially hazardous asteroids. One of those is the kinetic impactor, which involves a high-speed spacecraft that is designed to crash on target asteroid in order to steer it away from its orbital path to mitigate the risk of impact.[5)] Binary asteroids are ideal test beds to demonstrate capabilities of such techniques. Indeed, single asteroids are much more abundant, thus would likely be easier to target one, however it is much more challenging to observe changes in their orbit due to much longer period of motion. On the other hand, smaller companions in the binaries are orbiting their primaries in much shorter timescales; usually one or more orbits are completed less than a day. Hence, changes in an orbit after an impact would likely be much easier to observe.

The goal of the joint NASA/ESA multi-spacecraft mission proposal AIDA is to test the kinetic impactor technique in

Copyright© 2017 by the Japan Society for Aeronautical and Space Sciences and ISTS. All rights reserved.

the binary asteroid (65803) 1996GT Didymos.[4] Between two spacecraft proposed, NASA spacecraft Double Asteroid Redirection Test (DART) is planned to perform a high-speed impact on the smaller companion of Didymos, informally called Didymoon. Whereas ESA spacecraft Asteroid Impact Mission (AIM), whose future is now uncertain, tasked to observe pre- and post-impact variations on Didymoon orbit, as well as general properties of the binary system in order to understand the formation mechanism. AIM proposal also includes MASCOT-2 lander designed by German Aerospace Center, DLR and French Space Agency, CNES, to perform in-situ observations and two CubeSats to be deployed in the binary system in order to fulfill a secondary goal to test novel intersatellite communication techniques and enhance CubeSat heritage in interplanetary medium.[6] For the latter, ESA opened a call to the community in 2015 for novel CubeSat proposals.[6]

As a response to the call, the Royal Observatory of Belgium (ROB) proposed two 3U CubeSats to land on Didymoon, named as Asteroid Geophysical Explorer (AGEX) mission.[7] The first spacecraft (SeisCube) in the proposed concept includes a geophysical instrument package with a seismometer and a gravimeter to investigate subsurface properties. The second spacecraft (Bradbury) in fact carries a number of femtosats to be deployed throughout the surface, which are equipped with miniaturized instruments to investigate surface properties. Additionally, both CubeSats also accommodate same set of sensors in order to measure rotation and surface mechanical properties of Didymoon. The landing operation of the AGEX mission is foreseen to be fully passive, i.e. the proposed landing trajectories shall occur naturally, this is without the need of propulsive devices.

Such trajectories can be found in the Circular Restricted Three-Body Problem (CR3BP) dynamical model, in which the three bodies are the two binary companions and the lander spacecraft. In principle, these trajectories are driven only by natural dynamics, which means no active control on the trajectory is necessary. This then makes these trajectories ideal conduits for NanoSats or other small landers, that possess no, or only minimal control capabilities. It could also be a preferable solution for motherships, such as AIM, to deploy landers from a safer distance as the dynamical environment around asteroids imposes non-negligible risks to low-altitude landing operations. As a consequence, the research on delivering NanoSats, or science packages, on binary surfaces has gained a considerable interest.

Natural manifold deliveries of science packages on binary asteroids were studied by Tardivel and Scheeres previously.[8] They considered the vicinity of Lagrange points as deployment locations and defined first intersection of a trajectory with surface as landing. This work followed a strategy development for landings in binary asteroid 1996 FG_3, back-up target of Marco Polo-R mission proposal.[9] In a Monte Carlo analysis, they assessed the statistical success of landings. Moreover, within the context of MASCOT-2 lander, Tardivel et al.[10] discussed the passive landing opportunities on Didymoon, later with an additional optimization study carried out by Tardivel.[11] Along the same line, Ferrari carried out a trajectory design and Monte Carlo uncertainty simulation for MASCOT-2.[12] The study offered a landing strategy for ballistic landing based on Poincare maps with special emphasis on AIM proposal. In a recent study, Celik and Sanchez proposed a new technique to seek opportunities for ballistic soft landing in binary asteroids.[13] This technique defines a landing in local vertical and utilizes a bisection search algorithm to search minimum energy trajectories in a backwards propagation from the surface. In similar contexts, post-touchdown motion on asteroids was also tackled by several researchers.[14–16]

In the context of ROB's AGEX proposal, and on the groundwork of Celik and Sanchez, this paper focuses on a reliability analysis of ballistic landing for a CubeSat lander targeting Didymoon, under uncertainties and GNC errors by means of a Monte Carlo simulation. A spherical shape and point mass gravity are assumed for both binary companions, Didymain and Didymoon. A dense grid of landing points are created and distributed homogenously on the surface of the companions, whose locations are described by their latitudes and longitudes. Trajectories are then generated from each point by applying the methodology developed in Ref. 13). This allows us to obtain nominal trajectories under ideal conditions, as well as to generate an overview map of reachable regions and characteristics of landings on the surface as a function of landing location.

The generality of the methodology here provides a complete trajectory database for ballistic landings for each point in the grid. In principle, that allows evaluating successes for all regions of interest. Readily available trajectory database also contains useful information about trajectories, such as landing speeds. Landing speeds are the only parameter that defines characteristics of a trajectory along with predefined landing locations, as a consequence of local vertical landing. Thus, they can be modified to estimate the upper limit of required energy damping, or coefficient of restitution, in order to achieve higher success rates. Moreover, deployment locations are selected as the first intersection of a landing trajectory and an artificially defined safe distance from the binary barycenter, as a representative mothership location at the time of deployment. Thus, the analyses are not restricted to a certain distance, but can be generalized to greater or shorter distances of mothership from the barycenter, for all deployment locations.

Several, realistically defined uncertainty and error sources are randomly added to nominal trajectories. After a sufficient number of test cases are performed in a Monte Carlo simulation from corresponding deployment locations onto the surface, this paper aims to draw a preliminary conclusion about how non-ideal conditions might possibly affect touchdown success. This approach yields an overall picture of dispersion shape on the surface, as well as upper and lower boundaries for expected landing speeds, time durations and impact angles. Particularly, impact angles are treated as a simple criterion, due to definition of landings in local vertical, to assess relative robustness of trajectories. Furthermore, Monte Carlo success rates in all equatorial regions are also computed. This presents an overview about statistical success of landings in various equatorial longitudes under the assumptions provided.

2. Overview of Landing Trajectory Design

Suppose a mothership, in its operational orbit, orbiting at a safe distance from the binary systems barycentre. A passive

lander (or a NanoSat) can be sent onto the surface of one or the other binary companion from this mothership by exploiting the natural dynamics around the binary system. Landing trajectories in this dynamical scheme can be designed in the framework of Circular Restricted Three-Body Problem (CR3BP). In this setting, the third body (i.e. the lander CubeSat) moves under the gravitational attraction of its primary and secondary (i.e. Didymain and Didymoon) by having only negligible effect in return.[17] The dynamical model is traditionally derived in the rotational frame, whose center is at the barycenter of larger bodies, x-axis is on the line connecting them and z-axis pointing the normal of their mutual orbit plane.[17] Therefore, unless otherwise stated, the models and results will be provided in the rotational reference frame. CR3BP exhibits five equilibria, called Lagrange points (L1-L5), and five different regimes of motion, expressed in zero-velocity surfaces (ZVS).[17] For our notional mothership, an operational orbit can be defined in the exterior realm of ZVS, in which the L2 point is closed so that no natural motion is allowed to the interior realm. In this setting, L2 point presents the lowest energy gate to reach the interior region. Thus, a simple spring mechanism available on mothership can provide a gentle push to increase the landers energy in order to open up ZVS at L2 point and allow the motion to interior region.

The problem of landing trajectory design in such a scenario is tackled in the groundwork study performed by Celik and Sanchez in the context of a hypothetical binary asteroid.[13] In this study, landing is defined in the local vertical of a landing site, described by its latitude and longitude. Such description had the clear advantage of describing landing by only one parameter, i.e. landing (or touchdown) speed, $v_{landing}$, once a specific landing location is determined. Those initial state vectors are then propagated backwards from the surface to exterior region of ZVS in a specially developed bisection algorithm, inspired by Ren and Shan.[18] The algorithm searches for minimum energy landings in a reverse-engineered, iterative manner from the surface to exterior region of ZVS. This simple algorithm then allows trajectories to be designed for any arbitrary latitude-longitude pairs on the surface for any size of binary asteroids. Thus, it generates an overall picture for various features of landing, namely energies, speeds and coefficient of restitution (*CoR*) values. Moreover, after resulting trajectories are propagated sufficiently long time, multitudes of deployment points can be found on the path, for trajectory portions whose positions are beyond L2 point. It should be noted, that although spherical binary asteroid pairs are used, the methodology is general and can be applied to asteroids of any shape, in fact for all small bodies, as also done for the Philae's descent trajectory computation.[19]

A simulation was carried out with the algorithm, explained in the preceding paragraph, for landings in Didymoon. The results of landing speeds are provided in Fig. 1. Jacobi constant (i.e. energy) results are found to be less relevant to the analyses later, and therefore not provided.

In Fig. 1, 0^o represents the prime meridian whose point is arbitrarily defined as to be on x-axis, directly facing the L2 point; hence 0^o and 360^o correspond to same longitude. In general, L2 facing regions exhibit low energy characteristics, in agreement with the results for larger hypothetical binary.[13] Landings to those regions are possible with less than 10 cm/s, with the lowest being on the order of ~5 cm/s. About the half of Didymoon surface is reachable with such low energy landings. The results show a clear symmetry in latitudinal direction, while the same is not true for longitudinal direction, due to the rotation of Didymoon around its primary. It should also be noted that a region about 30^o-wide on the surface is not available for passive landings and marked as "no landing". Landings to that region are affected by the algorithm constraints, and would require to pass through the interior of Didymain.

Table 1. Properties of (65803) 1996GT Didymos.

Property	Didymain	Didymoon
Diameter [km]	0.775	0.163
Density [kg/m^3]	2146	
Mass [kg]	5.23 x 10^{11}	4.89 x 10^9
Mutual orbit radius [km]	1.18	
Mutual orbit period [h]	11.9	

As discussed earlier, the trajectory design technique also enables us to estimate *CoR* values on the surface. *CoR* in this study refers to the simple interaction between surface and a landing spacecraft with a specific value, similar to a bouncing ball on a surface and can be described in both local vertical and local horizontal. However, this paper only concerns with *CoR* values in local vertical, and assumes that the outgoing velocity is in the same plane as the incoming velocity and the surface normal vector. This may change due to surface features, such as boulders or rocks, however that is not considered here. *CoR* value then defines the energy dissipation due to surface properties, as in Eq. 1 in its simplest way.

$$\boldsymbol{v}_{LV}^{-} = (\hat{\boldsymbol{n}}.\boldsymbol{v}).\boldsymbol{v} \implies \boldsymbol{v}_{LV}^{+} = -CoR\boldsymbol{v}_{LV}^{-} \tag{1}$$

where subscripts (-) and (+) indicate incoming and outgoing speeds, respectively. *CoR* values must typically be between 0 and 1, but it may be considerably different in local horizontal and vertical directions.[14,21]

We can now compute *CoR* values to close ZVS at L2 point for landings depicted in Fig 1. Basically, this is a rough estimate of how much energy needs to be dissipated in a touchdown, so that motion of a lander CubeSat would be trapped near the binary system. It is clear that the same computation can also be performed for L1 and in fact the motion can be trapped around Didymoon, but our goal is to find the minimum dissipation necessary. Then, unless otherwise stated, *CoR* will always refer to the required energy dissipation to reduce the energy below that of L2 point. The results are provided in Fig. 2.

In a clear agreement with the results in Fig. 1, low energy regions show higher *CoR* values, hinting that very little energy dissipation would be enough to keep a lander near the binary system. In higher energy regions, *CoR* values begin to decrease to levels, for which a lander would likely to require an active landing system. Thus, for a purely passive landing, regions with low landing speed and high *CoR* appear to be more attractive options to consider. The focus of this study will therefore be those regions, even though results for other regions will also be presented. Hence, the values computed are essential to analyses in upcoming sections. For more detailed discussion, the reader may refer to the original work of Celik and Sanchez, or various

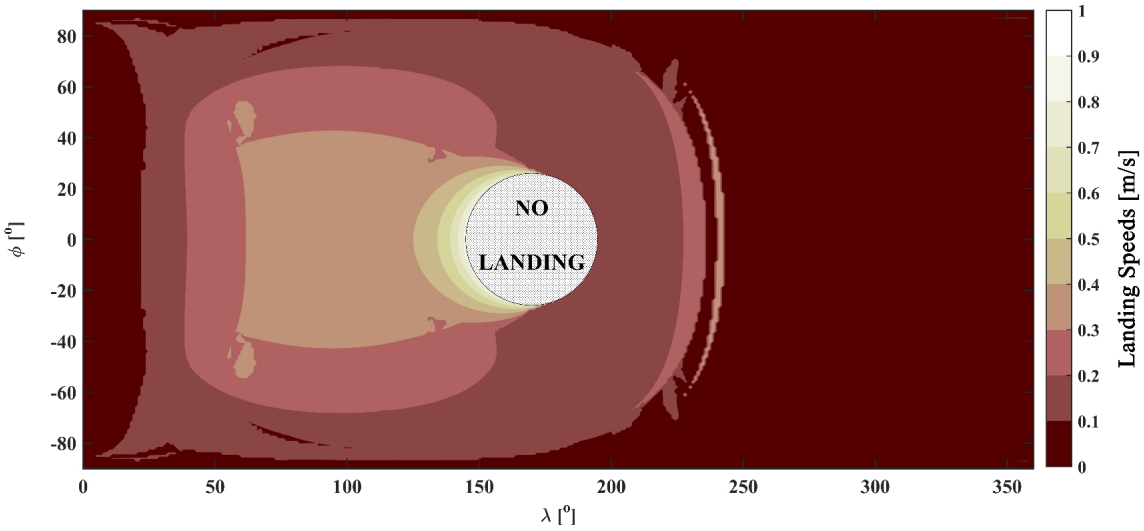

Fig. 1. Landing speeds on Didymoon surface.

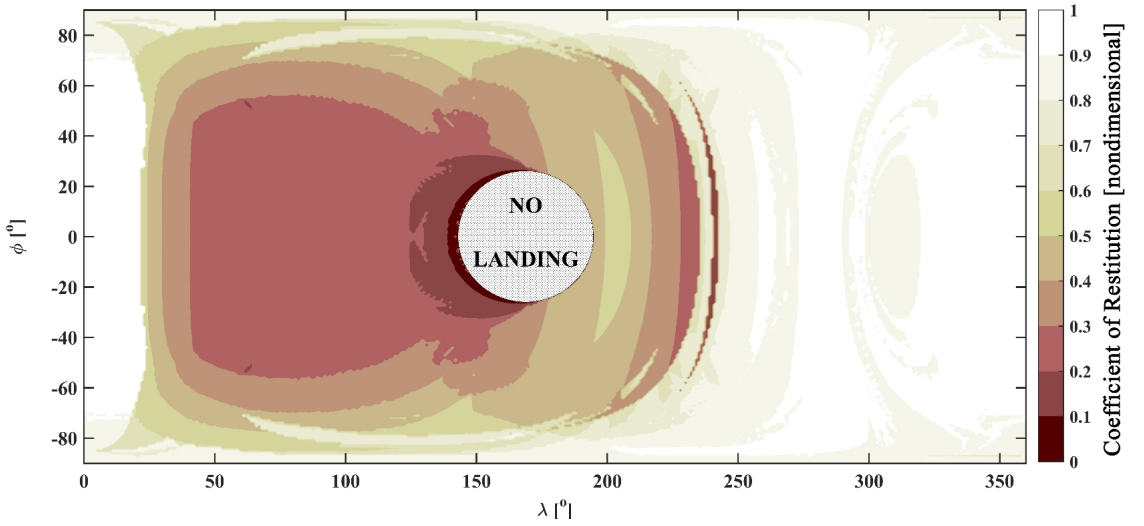

Fig. 2. Required energy damping (*CoR*) to close ZVS at L2 point.

others.[13–16,20,21]

Overall, although trajectories show a compelling prospect to be utilized as a landing strategy, their robustness is still in question. Particularly, trajectories are generated by this algorithm are largely idealized with relatively ad-hoc constraints,[13] and it is thus necessary to assess their robustness against non-ideal conditions.

3. Robustness Analysis: Monte Carlo Simulation

The generated nominal trajectories show promising landings for the CubeSat. However, most of low energy trajectories spend some time around L2 point before a touchdown. Then the question arises about their robustness against non-ideal conditions. A convenient way to test this is a Monte Carlo simulation, in which a large number of randomly generated samples is used to understand the overall statistical behavior of a system. Here, a Monte Carlo simulation is set up to assess the robustness of these trajectories, especially for those requiring lower energies. The simulation is restricted to equatorial landing trajectories (i.e. 2D).

3.1. Trajectory refining from the database

The nominal trajectory database is used to refine trajectories that are going to be used for Monte Carlo simulation. The trajectory information shown in Fig. 1 and 2 are obtained from 4 Didymos period simulations, i.e. about 2 days. This is a rather long term for landing operations, especially provided the fact that the CubeSat is unpowered and dynamical environment is highly uncertain. Thus, 12-h (i.e. one Didymos period) trajectory information is considered to be sufficient. This condition is established as the first criterion in trajectory refining process.

The second criterion is the minimum deployment altitude. Clearly, if the deployment altitude is lower, the landing (or at least, touchdown) success will likely to be higher. However, lower altitudes are rather unfavorable locations, where non-homogenous gravitational field of the Didymos system is more effective, and also close to the dynamically unstable equilibrium

point, L2. Bringing a mothership to this region might impose serious risks to mission operations. Hence, a minimum close approach distance is defined for the mothership, whose radius is measured from the barycenter along the x-axis as

$$r_{d,min} = d_{barycentre-moon} + r_{moon} + d_{safe} \tag{2}$$

where $r_{d,min}$ in Eq. 2 is the mothership close approach distance, $d_{barycentre-moon}$ is the distance from barycenter to Didymoon centre of mass, r_{moon} is Didymoon radius and d_{safe} is the safe distance for the mothership from the barycentre, which is a parameter that will be controlled. d_{safe} is selected 200 m as the minimum deployment altitude as for the initial analysis. Even though this altitude still seems close to the surface, it is beyond the L2 point of the system, hence can be deemed as relatively safe. A similar reasoning is also made during MASCOT-2 landing analysis.[23] The minimum close approach radius for the mothership, $r_{d,min}$, then adds up to 1451.6 m from the barycenter.

The first intersection of a trajectory with $r_{d,min}$ is considered to be the deployment location. It may happen that there could be other intersections over the course of one trajectory simulation, but they are simply neglected. Note that the choice of the first intersection (i.e. closest deployment location to the surface) results in different deployment altitudes based on the target longitude, when measured from the surface of Didymoon.

Above two criteria were initially applied to the trajectory database to extract possible deployment locations for various landing locations (defined by longitudes). Especially in the low energy regions, which are more of our interest, touchdown duration is much longer than 12 h from the minimum deployment altitude. As a result, less deployment opportunities exist with the above two criteria. Thus, if energy of trajectories can be increased, or in other words, if higher speeds can be tolerated in touchdown, faster trajectories can be obtained. This would be possible with an increase in landing speeds. A third criterion can then be defined in order to scale the speeds up in the surface:

$$v_{landing} = \frac{v_{L2}}{CoR} \tag{3}$$

where $v_{landing}$ is landing speed (i.e. resulting speed after the bisection search), v_{L2} is the necessary speed at a landing location to close L2 point to restrict the motion to interior realm and CoR is coefficient of restitution. v_{L2} is smaller than $v_{landing}$ by definition, hence using v_{L2} in the scaling process makes our CoR even more conservative. For instance, the landing speed $v_{landing}$ for 0^o longitude is 5.81 cm/s, and v_{L2} is 5.36 cm/s. When the latter is substituted in Eq. 3 to scale up $v_{landing}$ with a $CoR = 0.7$ assumption, the new landing speed becomes 7.66 cm/s. Consequently, it becomes as if the CoR value equals to ~0.75 if the nominal $v_{landing}$ value would have been used in Eq. 3, instead of v_{L2}.

Fig. 2 shows that in the L2-facing region, coefficient of restitution values may be higher than 0.9 for simple bouncing motion assumption. This is a very conservative, and possibly rather inaccurate estimation, in comparison to previous results obtained for the asteroid Itokawa (~0.85),[22] and the comet 67P/Churyumov-Gerasimenko (~0.7).[20] The studies for MASCOT-2 landing also considered values as low as 0.6 or even lower.[23] Hence, a CoR value of 0.7 is found to be conservative enough for this study. This value is then substituted in Eq. 3 to scale landing speeds. The value seems rather arbitrary; however, it is in the lower range of observed values in small bodies, and higher than the values considered for the MASCOT-2 landing analyses.

This new CoR value is fixed everywhere in the equatorial region. It is obvious that CoR values differ across the surface. Furthermore, there is also a region in Fig. 2, exhibiting much lower CoR values than 0.7, even lower than the value used for the MASCOT-2 landing analyses (~0.6).[23] It means that, by recomputing their $v_{landing}$ with $CoR = 0.7$, their energy is actually decreased. It is likely that some of the previously available deployment options will disappear for some of those longitudes. Although the results for those will also be provided, those are not our major regions of interest, since a landing to those would potentially require powered or semi-powered landers. We will restrict our attention to those that provide low energy, passive-landing prospects.

The choice of $CoR = 0.7$ makes trajectories remarkably faster and generally available for the first intersection within 12-h simulation. As an example, the trajectory targeting the prime longitude (i.e. 0^o), takes ~1.2 h to reach the first intersection. Before CoR modification, recall that the trajectory did not have enough the energy to reach the same point within 12 h.

Finally, a fourth constraint comes from the preceding study[13] and sets an upper bound of 2 m/s for maximum possible deployment speed. This upper bound is due to readily available technology for standardized CubeSat deployers.[24]

Then, the constraints formulated above can be summarized below:

- Release location must be searched within 12-h (one Didymos orbit) simulation time from the surface.
- d_{safe} must be no lower than 200 m altitude.
- Landing speeds need to be scaled up according to an expected CoR of 0.7.
- Maximum deployment speed must not exceed 2 m/s.

Consequently, trajectories that satisfy above constraints in the backwards propagation are selected for Monte Carlo simulation. Pseudo-random uncertainties and errors, that will be described in the next subsection, are then added to the refined nominal trajectories to run forwards from the deployment location, i.e. the first intersection of trajectories with the minimum circular orbit radius of the mothership, $r_{d,min}$.

3.2. Uncertainty and error sources

The uncertainty and error sources and their corresponding values can now be described. The mothership-related uncertainties are restricted to GNC errors, namely error in position and velocity of the mothership. An uncertainty sphere is defined for each with spacecraft in the center, and whose radii are defined by their 3σ values. On the other hand, the spring error is described in two parts, i.e. magnitude and angular errors. The angular error in the spring vector is in azimuth (α) and elevation (α), stretching to both positive and negative direction. The resulting spring vector then must be inside a wedge, whose dimensions are described by maximum error magnitude and angles $\pm\alpha$, $\pm\phi$.

Lastly, density errors associated with the binary system are considered. Didymos total system mass is known in a reasonable accuracy, as 5.28 x 10^{11} kg.[25] However, their individual masses and densities are not known exactly. Under our spherical asteroid and same density assumptions for both asteroid bodies, this breaks down into 5.23 x 10^{11} kg for Didymain and 4.89 x 10^{9} kg for Didymos, as in Table 1. As the system mass is known with a good accuracy, density error is only considered for Didymoon. However, Didymoon contribution to the total system mass is only ~1.2%, therefore it can be expected that density uncertainties of Didymoon would not be as effective as an uncertainty in Didymain or in total system mass. Those effects simply are not considered here and left for a possible future study. Table 2 below shows 3σ errors considered for Monte Carlo simulation.

Table 2. Uncertainty and error sources.

Source	3σ value
GNC position accuracy	15 m
GNC velocity magnitude accuracy	0.5 cm/s
Spring magnitude error	±30%
Spring angle error	$\pm 15^o$
Didymoon density uncertainty	±30%

Additionally, solar radiation pressure (SRP) is found to have a negligible effect on trajectories, mostly due to the short duration. Its effect is on the order of millimeter in position and 10^{-4}–10^{-5} mm/s in velocity.

Apart from the mentioned uncertainties and perturbations; surface properties, mass distribution, the exact shape of Didymoon and some other perturbations will certainly have an impact on touchdown location and velocities. However, these are simply not considered in this study. With regards to the shape, note that only epistemic uncertainties in the shape of the asteroid (i.e. inaccuracies on the final shape model) will affect the feasibility of the landing trajectories. In other words, the same procedure implemented here can be used with a more realistic shape model for Didymos, once this is known. Thus, only the errors in the final shape model will actually affect the trajectories, not the fact that at this stage a spherical shape is considered.

3.3. Simulation model

The Monte Carlo simulation model used here can be explained in three parts: first, refining trajectories from the database, second, generating pseudo-random uncertainty and error added trajectories, and third, trajectory propagation. Trajectory refining and uncertainty and error sources are explained in the previous two subsections. This section will discuss on how uncertainty- and error-added trajectories are generated from a nominal trajectory and effects of individual sources.

One of the advantages of reverse-engineered landing trajectories is their compact nature, providing a landing velocity vector on the surface. Then, after the bisection search, the resulting trajectory provides deployment velocities at possible deployment locations above the surface. This vector in reality is the sum of mothership orbital velocity and deployment spring velocity, as in Eq. 4, below:

$$\boldsymbol{v}_{deployment} = \boldsymbol{v}_{SC} + \boldsymbol{v}_{spring} \tag{4}$$

Here, $\boldsymbol{v}_{deployment}$ is the deployment velocity vector, $\boldsymbol{v}_{SC}$ is the mothership velocity vector and $\boldsymbol{v}_{spring}$ is the spring velocity vector.

Eq. 4 then allows us to consider and evaluate mothership- and spring-related uncertainties and errors separately, which would otherwise be rather difficult, and impossible to see their individual impacts on landing success. However, here we have an underdetermined problem with one known vector ($\boldsymbol{v}_{deployment}$), and two unknown vectors. Thus, in order to treat them individually, it is necessary to know or assume either $\boldsymbol{v}_{SC}$ or $\boldsymbol{v}_{spring}$, in addition to $\boldsymbol{v}_{deployment}$. It seems that $\boldsymbol{v}_{SC}$ is an easier target to make assumptions. The deployment operation will likely to include a close approach of the mothership in a hyperbola in barycentric inertial frame. In the closest approach, this can be translated as an instantaneous velocity in +y direction in rotational frame, due to an epicycle near L2 point, as also described in.[11] Assuming that the mothership will perform the deployment in the instant of the closest approach, $\boldsymbol{v}_{SC}$ can be defined by only assuming one parameter, i.e. velocity in +y direction in co-rotating frame, and whose magnitude is assumed as 2 cm/s. Then, Eq. 4 can be written in following form to obtain spring velocity, $\boldsymbol{v}_{spring}$:

$$\boldsymbol{v}_{spring} = \boldsymbol{v}_{deployment} - \boldsymbol{v}_{SC} \tag{5}$$

It is usually more difficult to design a definite spring velocity vector, as landing location is defined as a region rather then a target point. This shows yet another useful feature of backwards integration: as landing vector is defined for a certain landing location, then above Eq. 5 computes the spring velocity for that point. This then provides an accurate estimate of the spring velocity vectors for each landing point. If there is a landing region defined instead of a landing point, spring vectors for each landing point inside that region can easily be obtained.

After obtaining $\boldsymbol{v}_{spring}$, uncertainties and errors are going to be added to $\boldsymbol{v}_{spring}$ and $\boldsymbol{v}_{SC}$ to estimate new landing vectors that deviate from the nominal landing vector, defined as below:

$$\boldsymbol{v}_{deployment,u} = \boldsymbol{v}_{SC,u} + \boldsymbol{v}_{spring,u} \tag{6}$$

The subscript u in Eq. 6 is used to distinguish nominal trajectory from uncertainty- and error-added, deviated trajectories.

The uncertainties and errors are then inputted to a trajectory in a pseudo-random way, i.e. a randomly selected value is seeded for each trajectory from each bounded set of uncertainty sources. For each set of propagation, 1000 trajectories are generated by adding uncertainties and errors to nominal trajectories. Those are then propagated in forward time to the surface from the deployment location. A sufficient propagation time is allowed and an event function in the program is used to mark a touchdown.

The success criterion for our Monte Carlo simulation is determined as *touchdown*. The touchdown criterion is due to the fact that our simulation model is relatively simple, and no surface feature is considered to describe complex bouncing motion of a CubeSat. Then, *success rate* describes the percentage of trajectories that touch down Didymoon surface over 1000 sample trajectories. Trajectories that do not touch down on the surface

of either body over the course the simulation time are marked as *unsuccessful*.

It is now reasonable to investigate how individual sources, described in previous subsection, affects the success. Fig. 3 shows the results of individual sources in a Monte Carlo simulation for an example landing to the prime longitude. Recall that our analysis is restricted to equatorial trajectories.

It is easily noticeable in Fig. 3 that spring errors have a dominating effect, which causes the largest spread by itself. (Note that spring errors also include angle error.) Particularly, spring errors cause the largest spread in both latitudinal and longitudinal direction. Butterfly-like dispersion shape in Fig. 3 seems to be caused because of the constrained landing geometry. In this regard, the results here actually differ from some of the other studies that do not consider any specific landing geometry and obtain nominal trajectories directly in forward propagation.[8,12] The combination of spring errors with GNC velocity errors makes a very little difference, although seems to increase the spread slightly. Assuming an ideal spring, GNC errors define an elliptic region of landings around the target longitude. When only position errors are considered in GNC system while everything else is nominal, the dispersion does not change much, although shrinks slightly in longitudinal direction. Finally, density-only effects show a longitudinal dispersion, as can be expected from a point-mass induced gravity model, of about $\pm 10^o$.

3.4. Results

3.4.1. Landing target at 0^o latitude and 0^o longitude

The first Monte Carlo simulation is applied to a landing location at 0^o longitude and 0^o latitude. This point is the closest point to L2 and the point of the lowest energy landings. First, the trajectory refining process is applied to the nominal trajectory, and the first intersection of the refined trajectory with the closest approach distance of the mothership occurred at 239 m altitude above Didymoon surface. Then, a Monte Carlo analysis is carried out by applying the uncertainty models described previously and propagating the resultant sample of uncertain conditions forward in time. The success rate for this simulation is 99.9%, meaning that only one trajectory missed the surface or escaped before reaching it. The results can be seen in Fig. 4.

The dispersion shape is preserved compared to Fig. 3, suggesting that combined effect of all sources cannot diminish the effect of spring itself. Although slightly more scattered, maximum longitudinal dispersion does not magnify by the addition of other effects and the maximum touchdown longitude stays around 65^o longitude on the trailing side of Didymoon (negative longitudes) and about 50^o longitude on the leading side (positive longitudes). This longitudinal dispersion seems to be in an agreement with MASCOT-2 requirements,[23] and hence for AGEX, as it is proposed to be a "pre-cursor" of MASCOT-2.[26] This asymmetric longitudinal dispersion is closely associated with touchdown speeds on the surface. The grey "x" markers in Fig. 4 represent lower-than-average touchdown speeds (hereafter, lower speeds) whereas the black "+" markers represent higher-than-average touchdown speeds (hereafter, higher speeds). Even though each color can be seen in both sides, the grey and the black markers are mainly populated on the trailing and leading sides, respectively. Obviously, those lower speeds are the result of lower energy trajectories. In a straightforward reasoning, it can be inferred that the dispersion stretches farther in the trailing side, because those trajectories simply take longer to the surface after the separation, hence uncertainties and errors (especially those associated with angles) propagate longer. A similar reasoning can also be applied to higher speeds. They mostly populate within 25^o longitude from the nominal in the leading side, suggesting their higher speeds allow trajectory to reach the surface faster.

Compared to relatively wide and asymmetrical longitudinal variation, touchdown locations are in a narrower latitude range and almost symmetrical. All touchdowns occur roughly within $\pm 17^o$ latitudes. A vast majority, namely 91.3%, of trajectories touch down the surface in between $\pm 10^o$. Even though bouncing behavior of a CubeSat is rather unpredictable initially and heavily depends on touchdown conditions, it can be claimed that near-equatorial touchdowns would present a higher possibility to come to a rest within $\pm 60^o$ longitudes, which is defined to be maximum tolerable latitude for satisfactory illumination conditions for the mission.[23,26]

The results of touchdown speeds are presented in Fig. 4, in the upper right figure. Recall that the minimum vertical touchdown speed, $v_{landing}$ for this longitude is 5.81 cm/s, v_{L2} is 5.36 cm/s. Touchdown speeds are distributed roughly in the range between 5.5 cm/s to 10 cm/s, with their mean being 7.66 cm/s. Note in the figure the reference line at 12.3 cm/s, which shows one third of the estimated two-body escape speed of the Didymos system.[27] The maximum touchdown speed does not reach this point, suggesting that the CubeSat has a high chance to stay in the binary system after the touchdown.

In lower left corner of Fig. 4, time from release to touchdown is shown. As previously mentioned, the nominal trajectory reach the deployment altitude in ~1.2 h. The average time reach the surface is ~1.24 h, however relatively large number of trajectories reach the surface shorter than this, with the lowest being ~40 min. Those shorter trajectories are likely to be associated with the black "+" markers. In the other end of the figure, the time extends as long as 4 h, albeit with very low occurrence, which are likely to associated with lower speeds. It should be noted that resting of a CubeSat on the surface would take much longer than times shown here, as bouncing off the surface after touchdown is expected.

The last bar plot of Fig. 4 depicts impact angles in touchdown. That figure, in its present form, does not reveal much about touchdown conditions, as actual conditions strongly depend on surface properties and terrain. In this respect, it might even be preferable to land on shallower angles as comparing with vertical landing, if terrain has slopes. However, these results contain important information about trajectories itself, and the data can be interpreted in a different way. Since the landing geometry is defined in local vertical, amount of divergence from local vertical in touchdown may actually demonstrate the robustness of our trajectory design. The majority of touchdowns occur with impact angles within 15^o with respect to local vertical. The maximum occurring impact angles are lower than the average value, 12.25^o. Higher impact angles are also observed, though in much lower occurrences, up to 50^o for this case. Consequently, higher number of near-vertical landings in this Monte Carlo simulation suggests that the design of landing

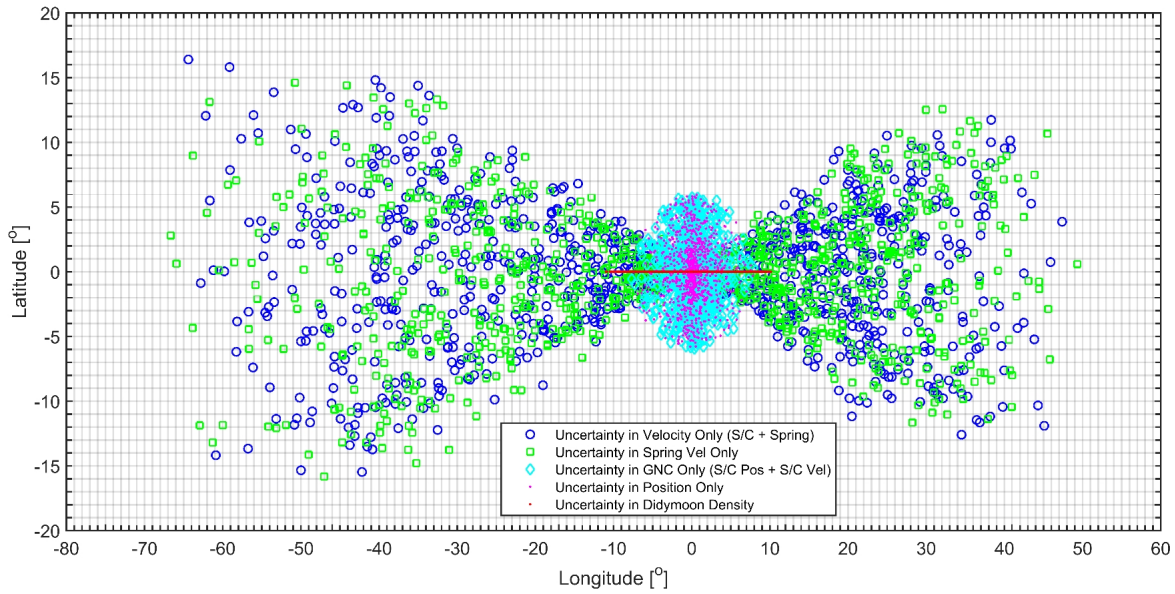

Fig. 3. The impact of individual sources on touchdown success.

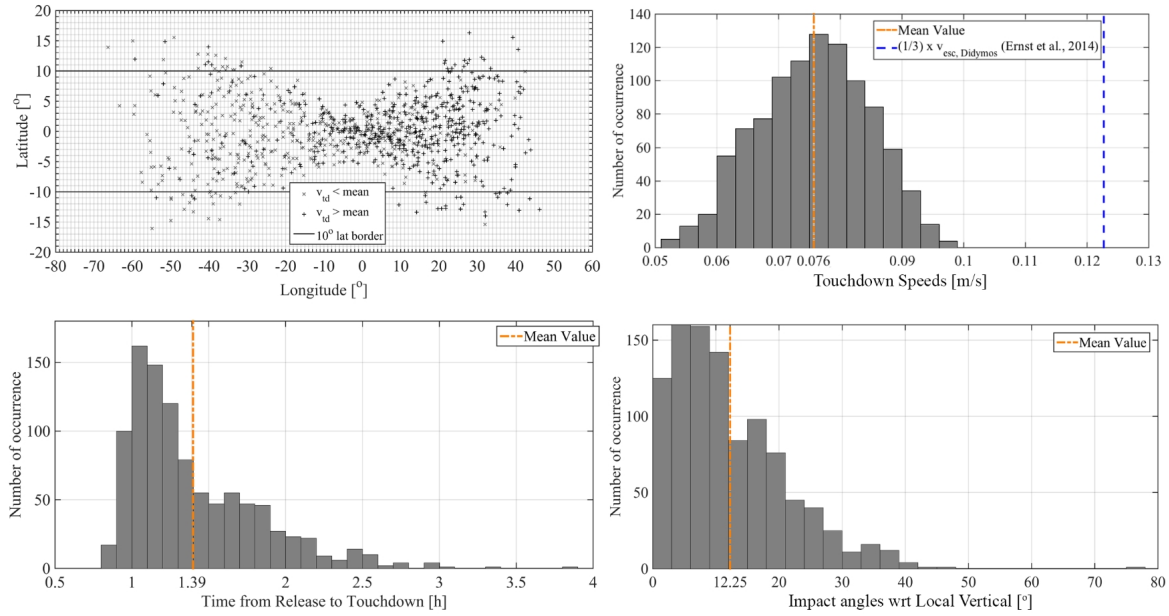

Fig. 4. The results of Monte Carlo simulation for landings to 0^o longitude.

trajectory is relatively robust for at least this landing.

The simulation presented a very high success rate for d_{safe} = 200 m. However, it is reasonable to investigate greater mothership distances in terms of touchdown success, as they are more preferable from risk assessment point of view for larger class missions. Table 3 provides the success rates of Monte Carlo simulation for various safe distances, d_{safe}, for the mothership, higher than 200 m.

Table 3. Success rates for various d_{safe}.

d_{safe}	Success rate
250 m	95.3%
300 m	76.1%
350 m	60.7%
400 m	57.1%

The results in Table 3 show a dramatic decrease in success rate as d_{safe} increases. The results of dispersion shape, the speeds, the angles, and the duration, which are presented in Fig. 4, are not provided for each d_{safe}, but it is straightforward to infer that dispersions would become wider and time-to-touchdown increases with increasing d_{safe}. Impact speeds tend to increase, however still below a third of escape speed of the system. Impact angles are also still in near-vertical range, though number of occurrences of shallower angles increases.

All in all, the Monte Carlo simulation for 0^o longitude shows a very high success rate, and offers a successful landing prospect with relatively low speed. Moreover, these results can confidently be extended for regions in which trajectories present similar low-energy characteristics. It means that these results cover almost about a sixth of all equatorial region of Didymoon surface, as illustrated in Fig. 1. It has been demonstrated that

for a successful touchdown to the lowest energy regions, trajectories need higher energies than their nominal. This might bring the discussion to bouncing behavior that is likely to occur. It is true that lower-speed landings are desirable to ensure to rest on the surface, but it apparently comes with an expense of risking a CubeSat not even reaching the surface, i.e. decreasing success rates. Furthermore, bounces may even be desirable in terms of mission success,[26] as gravity science instruments generally require multi-point measurements. Additionally, shorter touchdown duration after separation is also within design requirements of AGEX[26] (i.e., 2 h), despite the expected duration for resting on the surface is longer. Impact angle results present a robust performance for our trajectory design under given assumptions and uncertainty sources presented. Finally, an increase in deployment altitude has a severely degrading impact on touchdown success, whose value decreases to almost its half when the altitude is only doubled. It should particularly be noted that these results are not conclusive and as accurate as the simulation model, nonetheless, this fact does not attenuate the relevance and importance of the outcomes.

3.4.2. Landings at other Longitudes

It has been concluded that the results presented in previous subsection can be extended to other nearby longitudes. However, the extent of this claim, at least for equatorial region in question here, needs to be justified. For this part of the analyses, the minimum close approach distance of the mothership has not been changed, i.e. d_{safe} = 200 m. Also, *CoR* value and trajectory refining constraints have not been modified. As first intersection of a landing trajectory with the mothership distance is considered as the deployment location, landing trajectories that land on different longitudes will be deployed in different altitudes when measured from Didymos surface. This will of course have an impact on success rate as shown for the case in the previous section.

Overall Monte Carlo simulation results can now be investigated. In Fig. 5, target longitudes and deployment altitudes with their corresponding success rates, indicated by a color map, can be seen. In the figure, for instance, the deployment opportunity (i.e. the first intersection) for 0^o longitude occurs at about 240 m altitude from Didymoon surface, and it resulted in a success rates between 90-100% as an estimate. Note the actual success rate is 99.9%. The diagonal texture in the middle represents longitudes where no deployment opportunities occur with the criteria explained previously. Recall that the cause of this is partially due to the choice of $CoR = 0.7$. Thus, it can be inferred that approximately half of the equatorial region is available for deployment with the provided criteria, albeit with varying success rates. Among them, approximately 60^o-wide region in the L2-facing side present over 90% success with about half of them over 98%.

Fig. 5 also demonstrates success rate trends associated to an unexpected behaviour near L2 point. Around longitudes between 25^o–35^o, success rates do not follow a continuous trend and are increasing and decreasing again despite increasing deployment altitude. Around 30^o, the incomplete revolutions around L2 results in more touchdowns on the opposite side of Didymoon than any other nearby target longitude, hence higher success rates are observed, even though deployment altitude is higher. All in all, however, success rates on the trailing side show much more predictable behavior compared to that of in the leading side.

4. Conclusion

This paper has investigated the robustness of trajectories by means of Monte Carlo simulations, to successfully send a CubeSat onto the surface of the smaller companion of Didymos. Building a model on top of a previously developed algorithm, various simulations have been carried out in order to assess statistical success of nominal trajectories, which are obtained in ideal conditions, under the effect of uncertainties and GNC errors. It is found, that touchdown successes are strongly related to the deployment distance, and the constrained landing geometry.

The backward integration technique is successfully utilized to obtain a nominal trajectory database. Several realistic, easily modifiable criteria are applied to refine the database to finally extract trajectories to be used in the simulation. It was found, that target low energy regions are considerably slow to reach surface, thus unavailable for shorter landing operations and prone to suffer from uncertainties. A simple scale-up process is applied to landing speeds in order to increase their energy by means of assuming a new, conservative coefficient of restitution, whose value is in harmony with observations and theoretical analyses. This modification allowed a greater number of trajectories to be available for Monte Carlo simulation.

Realistically defined uncertainties and errors are added to refined trajectories and a sufficient number of trajectories is propagated to the surface in forward time. The results show, that for low energy regions present higher touchdown success rates than higher energy regions. However, higher success rates for low energy regions are strictly limited to low altitudes. Touchdowns mostly occur in near-equatorial latitudes, though with much wider longitudinal dispersion. It was found, that the dispersion shape on the surface is affected due to the constrained landing geometry, i.e. in local vertical, and in this respect it differs from some of the results in the literature. Impact speeds are always lower than the escape speed of Didymos. Near vertical impact angles are proven as a useful relative measure of robustness of trajectory design. Monte Carlo results for all equatorial longitudes show that high success rates are not limited to only few longitudes.

To conclude, it should be noted that Monte Carlo analyses carried out here only represent only statistical success rates of vertical landings, designed in the backwards integration approach. Different landing conditions may exhibit more successful deployment conditions. Similarly, an extension of the simulation into a spatial case may also reveal more regions to be reached with higher success rates.

Acknowledgments

Onur Celik is supported by the ROB Dynamics of Solar System Short-Term Research Grant for this particular study. He is also a MEXT Scholar, supported by Japanese Government (Monbukagakusho) Scholarship for his research in Japan.

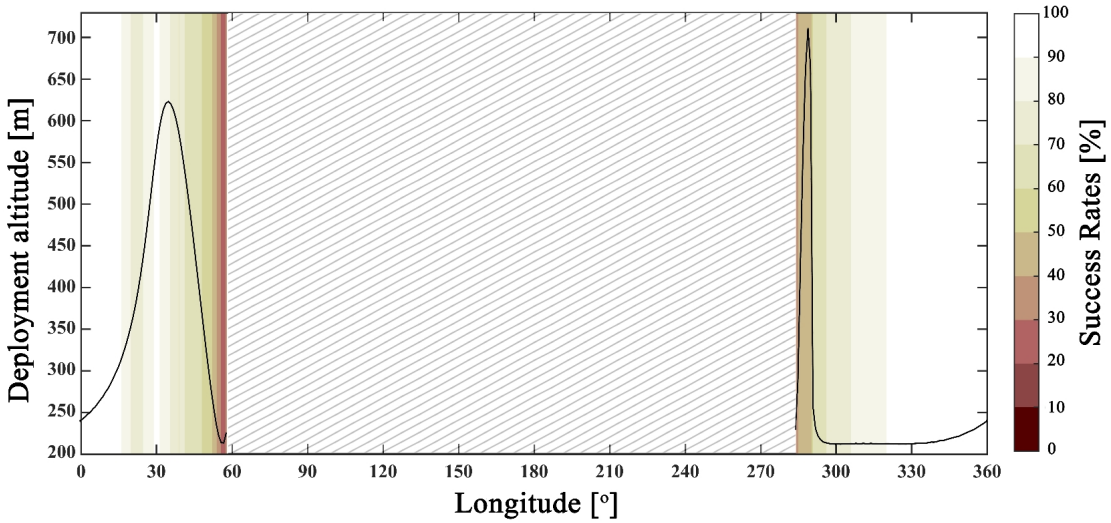

Fig. 5. Overall Monte Carlo results for all target sites available.

References

1) Margot, J. L., Nolan, M. C., Benner, L. a. M., Ostro, S. J., Jurgens, R. F., Giorgini, J. D., and Campbell, D. B.: Binary asteroids in the near-Earth object population, *Science*., **296** (2002), pp.1445–1448.
2) Barucci, M. A., Cheng, A. F., Michel, P., Benner, L. A. M., Binzel, R. P. , Bland, P. A., and Zolensky, : MarcoPolo-R near earth asteroid sample return mission, *Experimental Astronomy*., **33** (2012), pp.645–684.
3) Anderson, R. C., Scheeres, D., Chesley, S., and the Basix Science Team: Binary Asteroid in-situ Explorer Mission (BASiX): A Mission Concept to Explore a Binary Near Earth Asteroid System, 45th Lunar and Planetary Science Conference, The Woodlands, Texas, LPI Contribution No. 1777, 2014.
4) Cheng, A. F., Atchison, J., Kantsiper, B., Rivkin, A. S., Stickle, A., Reed, C., and Ulamec, S.: Asteroid Impact and Deflection Assessment mission. *Acta Astronautica*, **115** (2015), pp. 262–269.
5) Sanchez, J. P. and Colombo, C.: Impact hazard protection efficiency by a small kinetic impactor., *Journal of Spacecraft and Rockets*., **50** (2013), pp. 380–393.
6) Carnelli, I., Galvez, A. and Walker, R.: Science by Cubes: Opportunities to Increase AIM Science Return, 4th Interplanetary CubeSat Workshop, London, UK, iCubeSat 2015.B.1.3., 2015.
7) Karatekin, O., Mimoun, D., Murdoch, N., Ritter, B. and Gerbal, N.: The Asteroid Geophysical EXplorer (AGEX) to explore Didymos, 5th Interplanetary CubeSat Workshop, Oxford, UK, iCubeSat 2016.A.2.1., 2016.
8) Tardivel, S., and Scheeres, D. J.: Ballistic Deployment of Science Packages on Binary Asteroids, *Journal of Guidance, Control, and Dynamics*, **36** (2013), pp. 700–709.
9) Tardivel, S., Michel, P. and Scheeres, D. J.: Deployment of a lander on the binary asteroid (175706) 1996 FG_3, potential target of the european MarcoPolo-R sample return mission, *Acta Astronautica*, **89** (2013), pp. 60–70.
10) Tardivel, S., Lange, C., Ulamec, S., and Biele, J.: The Deployment of MASCOT-2 to Didymoon, 26th AAS/AIAA Space Flight Mechanics Meeting, Napa, California, AAS 16-219, 2016.
11) Tardivel, S.: Optimization of the Ballistic Deployment to the Secondary of a Binary Asteroid, *Journal of Guidance, Control, and Dynamics*, **39** (2016), pp. 2790–2798.
12) Ferrari, F.: Non-Keplerian Models for Mission Analysis Scenarios about Small Solar System Bodies, Ph.D. Thesis, Politecnico di Milano, 2016.
13) Celik, O. and Sanchez, J. P.: Opportunities for Ballistic Soft Landing in Binary Asteroids, *Journal of Guidance, Control, and Dynamics*, ahead of print (2017).
14) Tardivel, S., Scheeres, D. J., Michel, P., van Wal, S., and Sanchez, P.: Contact Motion on Surface of Asteroid, *Journal of Spacecraft and Rockets*, **51** (2014), pp. 1857–1871.
15) Sawai, S., Kawaguchi, J., Scheeres, D. J., Yoshikawa, N., and Ogasawara, M.: Development of a Target Marker for Landing on Asteroids, *Journal of Spacecraft and Rockets*, **38** (2001), pp. 601–608.
16) Kubota, T., Sawai, S., Hashimoto, T., and Kawaguchi, J.: Collision dynamics of a visual target marker for small-body exploration, *Advanced Robotics*, **38** (2007), pp. 1635–1651.
17) Szebehely, V.: *Theory of Orbits*, Academic Press, New York, 1967.
18) Ren, Y., and Shan, J.: A novel algorithm for generating libration point orbits about the collinear points. *Celestial Mechanics and Dynamical Astronomy*, **120** (2014), pp. 57–75.
19) Canalias, E., Blazquez, A., Jurado, E., and Martin, T.: Philae Descent Trajectory Computation and Landing Site Selection on Comet Churymov-Gerasimenko. Proceedings of International Symposium on Spaceflight Dynamics, Laurel, Maryland, USA, 2014.
20) Biele, J., , Ulamec, S., Maibaum, M., Roll, R., Witte, L., Jurado, E., Munoz, P., Arnold,W., Auster, H.-U., and Casas, C.et al.: The Landing(s) of Philae and Inferences About Comet Surface Mechanical Properties, *Science*, **349** (2015), pp. 1–6.
21) Ulamec, S., Fantinati, C., Maibaum, M., Geurts, K., Biele, J., Jansen, S., and ORourke, L.: Rosetta Lander–Landing and Operations on Comet 67P/ChuryumovGerasimenko, *Acta Astronautica*, **125** (2016), pp. 80–91.
22) Yano, H.,Kubota, T., Miyamoto, H., Okada,T., Scheeres, D., Takagi,Y., Yoshida, K., Abe, M., Abe, S., and Barnouin-Jha, O.: Touchdown of the Hayabusa Spacecraft at the Muses Sea on Itokawa, *Science*, **312** (2006), pp. 1350–1353.
23) Ho, T., Biele, J. and Lange, C. : AIM MASCOT-2 Asteroid Lander Concept Design Assessment Study, DLR Executive Summary v1.0, 2016.
24) Pignatelli, D.: Poly Picosatellite Orbital Deployer Mk. III Rev. E User Guide, California Polytechnic State Univ., CP-PPODUG-1.0-1, 2014.
25) European Space Agency (ESA): Asteroid Impact Mission: Didymos Reference Model, http://emits.sso.esa.int (April 12, 2017).
26) Karatekin, O., Ritter, B., Mimoun, D., Murdoch, N., Cadu, A., Carrasco, J., Quiros, J. G., Vasseur, H., Larock, V., Tardivel, S., Rambaux, N., Ranvier, S., deKeyser, J., Yyseboodt, M., Dehant, V., and Gerbal, N.: SysNova COPINS Asteroid Geophysical Explorer: AGEX Challenge Analysis Draft Final Report, 2016.
27) Ernst, C. M., Barnouin, O. S., Stickle, A. M.: Analytical Calculations of Ejecta Mass and Crater Size Produced by the Impact of the DART Spacecraft into the Moon of Didymos, AIDA International Workshop, Maryland, USA, 2014.